2009 American Control Conference
Hyatt Regency Riverfront, St. Louis, MO, USA
June 10-12, 2009

State-Dependent Trajectory Planning and Tracking Control of Unmanned Surface Vessels

Reza A. Soltan, Hashem Ashrafiuon, and Kenneth R. Muske
Center for Nonlinear Dynamics and Control, Villanova University, Villanova, PA 19085

Abstract— **A new method combining trajectory planning, tracking and coordinated control for unmanned surface vessels is presented based on nonlinear sliding mode control. A limiting factor of sliding mode tracking control is that it can only guarantee position tracking as long as the vessel initial conditions are on the desired trajectory. In this work, a transitional trajectory between the vessel initial condition and the desired trajectory path is implemented using a set of two ordinary differential equations (ODEs) in terms of the position state feedbacks such that the ODE solution converges to the desired trajectory path. An additional advantage of this approach is that when the ODE represents a limit cycle, it can be used for coordinating multiple vessel trajectories without any possibility of collision. Several simulations are presented where the vessel successfully reaches and follows a desired trajectory starting from a variety of initial starting conditions.**

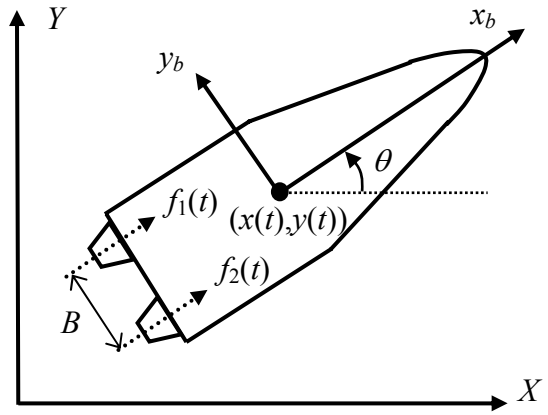

Fig. 1. Planar model of a surface vessel with two propellers

I. Introduction

Nonlinear position control of underactuated vehicle systems is an interesting and complex research topic due to modeling uncertainties, underactuation, and only indirect control of in-tracking variables through the nonholonomic constraints in the equations of motion. For example, consider the planar model of a surface vessel shown in Fig. 1. The control inputs from the two propellers can only provide a surge motion and planar rotation. The difficulty arises from the fact that only one input (total surge force) will appear in the two nonlinear differential equations representing the horizontal and vertical motion. Hence, tracking a path or trajectory is only possible with the aid of the yaw rotation where the mathematical formulation of the control problem becomes nontrivial.

Application of underactuated control approaches to unmanned surface vessels (USV) may be divided into set point [1-6] and trajectory tracking [7-19] position control problems since the respective controllers are different. In general, tracking control may only be possible if the trajectory to be followed does not include all three position variables simultaneously. In other words, the USV position can be tracked precisely while the heading angle is uncontrolled, i.e. the desired trajectory does not include a desired heading angle. In our previous work, such a control law was developed where simple straight line or curved desired trajectories were considered [17-18]. Further, the control law required the vessel's initial conditions to be on the desired trajectory. The design of a new trajectory planning and tracking controller for position control of a USV from an initial point to a prescribed desired trajectory is presented in this work.

The paper is organized as follows. The kinematic and dynamic model of the vessel shown in Fig. 1 is presented. Based on this model, an asymptotically stable trajectory tracking sliding mode control law is presented using two sliding surfaces for calculation of the two propeller forces. The first sliding surface is a first order surface comprised of position and velocity tracking errors of the surge motion. The second surface is second order and defined in terms of the vessel's lateral position, velocity, and acceleration tracking errors. Since the resulting control law requires the initial conditions to be on the desired trajectory, a new transitional trajectory is planned using a set of two ODE's. The two states of this trajectory are defined in terms of the position state feedbacks, while their dynamics are determined by the ODE's. The solution of these ODE's provides a smooth transition from any set of initial conditions to a desired target trajectory. Hence, the ODE's steady-state solution is the target trajectory. This target can be defined as periodic type trajectories that arise from stable limit cycles or fixed set points. An additional advantage of this approach is that when the ODE represents a limit cycle, it can be efficiently used for coordinated control of several vessels without any possibility of collision. For this purpose, the same ODE is used to generate the trajectories for all USV's starting from different initial conditions (time or position). The trajectories can never collide because the ODE must satisfy the existence and uniqueness conditions of the solution for the limit cycle. Several simulations are presented where the vessel reaches and then follows a desired circular trajectory at a constant speed or a set point starting from different initial conditions.

978-1-4244-4524-0/09/$25.00 ©2009 AACC

II. NONLINEAR USV MODEL

The three degree of freedom planar model of the USV shown in Fig. 1 is considered in this work. The USV is underactuated with two propeller force inputs $f_1(t)$ and $f_2(t)$ a distance B apart. The surge force $f(t)$ and steering torque $T(t)$ delivered by the two propeller forces are derived from the propeller forces as

$$f(t) = f_1(t) + f_2(t), \quad T(t) = \frac{B}{2}(f_2(t) - f_1(t)) \tag{1}$$

The kinematic relations between the inertial reference frame (X, Y) and the vessel-based body-fixed frame (x_b, y_b) are

$$\begin{aligned} \dot{x}(t) &= v_x(t)\cos\theta(t) - v_y(t)\sin\theta(t) \\ \dot{y}(t) &= v_x(t)\sin\theta(t) + v_y(t)\cos\theta(t) \\ \dot{\theta}(t) &= \omega(t) \end{aligned} \tag{2}$$

In the body-fixed frame, the nonlinear equations of motion may be written as

$$\begin{aligned} & m_{11}\dot{v}_x(t) - m_{22}v_y(t)\omega(t) + d_{11}v_x^{\alpha_1}(t) = f(t) \\ & m_{22}\dot{v}_y(t) + m_{11}v_x(t)\omega(t) + d_{22}\,\mathrm{sgn}(v_y(t))\left|v_y(t)\right|^{\alpha 2} = 0 \\ & m_{33}\dot{\omega}(t) + m_d v_x(t)v_y(t) + d_{33}\,\mathrm{sgn}(\omega(t))\left|\omega(t)\right|^{\alpha_3} = T(t) \end{aligned} \tag{3}$$

where $m_d = m_{22} - m_{11}$ and $m_{22} \neq m_{11}$ due to the added mass effect. The hydrodynamic damping is modeled as power law with exponents α_i and coefficients d_{ii}, i=1,2,3. Note that only forward motion dynamics are considered. More details on the USV model derivation and relations are presented in [17] and [18].

III. CONTROLLER DESIGN

The controller is based on the sliding mode control law where the desired state trajectory is described by a nonlinear dynamic system as follows

$$\dot{x}_i(t) = h_i(x_1(t), x_2(t)), \quad h_i : D_i \to R^2, \quad i = 1,2 \tag{4}$$

where $x_1(t)$ and $x_2(t)$ are the state variables of the desired system trajectory, D_i is an open and connected subset of R^2, and h_i is a locally Lipschitz map from D_i into R^2. Therefore, Eq. (4) represents the desired closed-loop system dynamics or vessel trajectory in this paper.

In the sliding mode control approach, a set of asymptotically stable surfaces (S) are defined as functions of the tracking errors such that all system trajectories converge to these surfaces in finite time and slide along them until they reach the desired destination at their intersection. The reaching conditions are established by defining $\frac{1}{2}S^T S$ as the Lyapunov function and ensuring that for surface i [20]:

$$S_i\dot{S}_i \le -\eta_i\left|S_i\right|, \quad \eta_i > 0 \tag{5}$$

where the value of the constants η_i (effort parameters) determine how fast the trajectory will reach surface i.

In the case of underactuated surface vessels, two surfaces in terms of the surge and lateral velocities are defined to determine the two control inputs. The desired state trajectories in the inertial reference frame are related to the desired surge and lateral velocity and acceleration as:

$$\begin{aligned} v_{xd}(t) &= \cos\theta(t)\,\dot{x}_1(t) + \sin\theta(t)\,\dot{x}_2 \\ \dot{v}_{xd}(t) &= \cos\theta(t)\,\ddot{x}_1(t) + \sin\theta(t)\,\ddot{x}_2(t) + v_{yd}\omega(t) \end{aligned} \tag{6a}$$

$$\begin{aligned} v_{yd}(t) &= -\sin\theta(t)\,\dot{x}_1(t) + \cos\theta(t)\,\dot{x}_2 \\ \dot{v}_{yd}(t) &= -\sin\theta(t)\,\ddot{x}_1(t) + \cos\theta(t)\,\ddot{x}_2(t) - v_{xd}\omega(t) \end{aligned} \tag{6b}$$

A. Surge Control Law

The first sliding surface is a first order surface defined in terms of the vessel's surge motion tracking error

$$S_1(\tilde{v}_x) = \tilde{v}_x(t) + \lambda_1\textstyle\int_0^t \tilde{v}_x(\tau)d\tau \tag{7}$$

where "~" is used to denote the tracking errors which is the difference between the actual and desired values; i.e. $\tilde{v}_x(t) = v_x(t) - v_{xd}(t)$. Note that $v_{xd}(t)$ is expressed in terms of $\dot{x}_1(t)$ and $\dot{x}_2(t)$, as shown in Eq. (6). The values of $\dot{x}_1(t)$ and $\dot{x}_2(t)$ can either be computed from a desired state trajectory $\dot{x}_d(t)$ and $\dot{y}_d(t)$ as proposed in [17], or from Eq. (4) in terms of the state position feedbacks $x(t)$ and $y(t)$:

$$\dot{x}_i(t) = h_i(x(t), y(t)), \quad i = 1,2 \tag{8}$$

Taking the time derivative of the surface and using the first relationship in Eq. (3), the surge control input can be determined as:

$$f(t) = f_s - k_s\,\mathrm{sgn}(S_1(\tilde{v}_x(t))) \tag{9}$$

where the terms

$$\begin{aligned} f_s &\equiv f_s(v_x(t), v_y(t), \omega(t), v_{xd}(t), \dot{v}_{xd}(t)) \\ k_s &\equiv k_s(v_x(t), v_y(t), \omega(t), v_{xd}(t), \dot{v}_{xd}(t)) \end{aligned}$$

are derived based on the nominal model and its uncertainty bounds as presented in [17]. Note that, the wave and wind forces may also be modeled [20] with their uncertainties and accounted for in Eq. (9).

B. Lateral Motion Control Law

We define the second sliding surface as a second-order surface in terms of the vessel's lateral motion tracking errors

$$S_2(\tilde{v}_y, \dot{\tilde{v}}_y) = \dot{\tilde{v}}_y(t) + 2\lambda_2 \tilde{v}_y(t) + (\lambda_2)^2 \int_0^t \tilde{v}_y(\tau) d\tau \quad (10)$$

where $\tilde{v}_y(t) = v_y(t) - v_{yd}(t)$ and $\dot{\tilde{v}}_y(t) = \dot{v}_y(t) - \dot{v}_{yd}(t)$. Derivation of the time derivative of the second surface requires $\ddot{v}_y(t)$. Hence, taking the time derivative of the lateral equation of motion in Eq. (3) and substituting for the accelerations from the surge and yaw equations, the yaw moment control can be calculated. The yaw control moment is derived as a function of the surge control force as:

$$T(t) = f_y - k_y \operatorname{sgn}(S_2(\tilde{v}_y(t), \dot{\tilde{v}}_y(t))) \quad (11)$$

where

$$f_y \equiv f_y(v_x(t), v_y(t), \omega(t), v_{xd}(t), v_{yd}(t), \dot{v}_{xd}(t), \dot{v}_{yd}(t), \ddot{v}_{yd}(t), f(t))$$

and

$$k_y \equiv k_y(v_x(t), v_y(t), \omega(t), v_{xd}(t), v_{yd}(t), \dot{v}_{xd}(t), \dot{v}_{yd}(t), \ddot{v}_{yd}(t), f(t))$$

are derived based on the nominal model and its uncertainty bounds as presented in [17]. Note that the wave and wind moments may also be modeled and their uncertainties can be accounted for in Eq. (11) through these terms.

IV. Stability Analysis

Proposition 1. The sliding mode control law for the surge force and yaw moment presented in Eqs. (9) and (11) is an asymptotically stabilizing trajectory tracking controller for the desired system trajectory represented by Eq. (4).

Proof. The surge and yaw controls presented in Eqs. (9) and (11) are derived based on the reaching conditions in Eq. (5) and hence guarantee that the system trajectory reaches the surfaces defined in Eqs. (7) and (10) in finite time [19, 21]. Further, the two surfaces are exponentially stable. Hence, the system trajectory asymptotically slides to their origin:

$$\tilde{v}_x(t) \,\&\, \tilde{v}_y(t) \to 0 \Rightarrow v_x(t) \to v_{xd}(t) \,\&\, v_y(t) \to v_{yd}(t) \quad (12)$$

Using the homogeneous transformation of Eq. (2) to obtain $v_x(t)$ and $v_y(t)$ and subtracting Eq. (6) from these values, the following relationships

$$\dot{x}(t) \to \dot{x}_1(t) \quad \& \quad \dot{y}(t) \to \dot{x}_2(t) \quad (13)$$

follow from the relationships shown in Eq. (12). Hence, the USV will track the desired dynamic system trajectory defined by Eq. (4) since $x_1(t)$ and $x_2(t)$ are the set equal to the position state feedbacks, i.e. $x_1(t) = x(t)$ and $x_2(t) = y(t)$. □

Remark 1. The yaw control moment presented in Eq. (11) has a singularity when the vessel is not in motion, i.e. when $v_x(t) = 0$.

Proposition 2. The rotational motion of the vessel is BIBO stable under the sliding mode control law.

Proof. Let us define the Lyapunov candidate function

$$V = \frac{1}{2} m_{33} \omega^2 \quad (14)$$

Using Eq. (3), the time derivative of V may be written as:

$$\begin{aligned} \dot{V} &= \omega(t)\left[T(t) - m_d v_x(t) v_y(t) - d_{33} \operatorname{sgn}(\omega(t)) |\omega(t)|^{\alpha_3} \right] \\ &= \omega(t)\left(T(t) - m_d v_x(t) v_y(t)\right) - d_{33} |\omega(t)|^{1+\alpha_3} \end{aligned} \quad (15)$$

Hence, $\dot{V} < 0$ if $d_{33}|\omega(t)|^{\alpha_3} > T(t) - m_d v_x(t) v_y(t)$. Since for any bounded desired trajectory defined in Eq. (4), $T(t)$, $v_x(t)$, and $v_y(t)$ will be bounded due to the control law's asymptotic stability, then $\omega(t)$ remains bounded since large ω values will make V a Lyapunov function.

V. Trajectory Planning and Simulations

The control law developed in our previous work [17-18] required the starting point to be on the desired trajectory and trajectories were expressed explicitly in terms of time and boundary conditions. However, this approach is not feasible in many applications. For example, it is physically difficult to start on a constant speed circular trajectory. A possible solution is to plan an initial trajectory using arcs and straight lines such the vessel will join such a desired trajectory [8]. However, this approach can result in a discontinuous control that may not be achievable due to actuator limitations. In this work, a smooth transition to the desired trajectory can be achieved through the use of trajectories defined in terms of ordinary differential equations. These transitional trajectories use the actual position state (x, y) feedback to converge to the target desired trajectory. Examples of such trajectories are closed periodic orbits including limit cycles and fixed position set points.

A. Simulations with Isolated Periodic Orbits

In this example, the USV is required to converge to an isolated orbit (limit cycle) with origin (x_o, y_o) starting from any set of initial conditions. The dynamic system describing the desired state trajectory is

$$\begin{cases} \dot{x}_1(t) = +w(t) x_2(t) - a_1 x_1(t)[g(x_1(t), x_2(t))] \\ \dot{x}_2(t) = -w(t) x_1(t) - a_2 x_2(t)[g(x_1(t), x_2(t))] \end{cases} \quad (16)$$

where $x_1(t) = x(t) - x_\circ$ and $x_2(t) = y(t) - y_\circ$ are the state variables of the desired trajectory, $g(x_1(t), x_2(t)) = 0$ is the equation of the continuously differentiable closed orbit, a_1 and a_2 are positive constants, and $w(t) \neq 0$ is a continuous time function that must converge to the desired angular velocity of the vessel on the closed orbit prior to reaching the orbit. This function must remain positive for counter clockwise rotation around the orbit and negative for clockwise rotation before reaching its constant value.

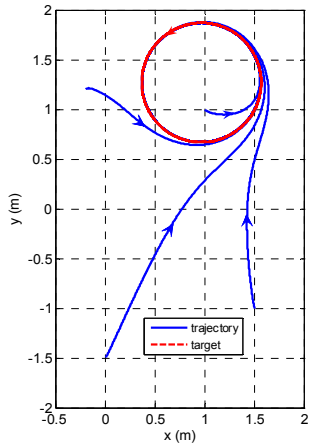

Fig. 2. Trajectory tracking from four different starting points for the circular-orbit target

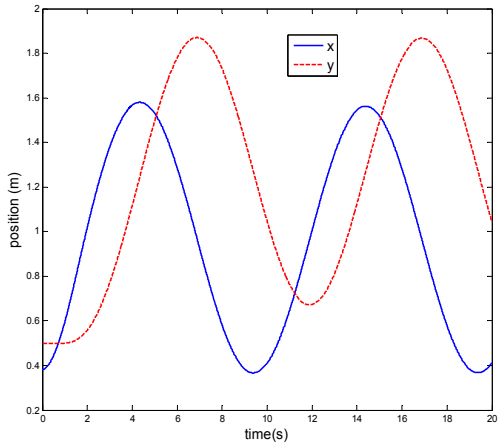

Fig. 3. USV position time history in inertial reference frame for reaching and tracking the circular orbit

Parameters a_1, a_2, and $w(t)$ must be adjusted according to actuator saturation or experimental implementation. For simulation purposes, however, it can always be assumed that $a_1 = a_2 = 1$ and $w(t)$ = constant desired angular velocity around the closed orbit. An example of such a closed orbit is a circle with a radius r similar to the unit radius circle presented in [22]:

$$g(x_1(t), x_2(t)) = x_1^2(t) + x_2^2(t) - r^2$$

The solution to Eq. (17) is a stable limit cycle where all trajectories converge to a circle of radius r and origin (x_o, y_o) except the one trajectory starting from the circle's origin which is an unstable equilibrium point.

In the simulations, the USV model with B = .07m and the following data and uncertainty in SI units is used [19]:

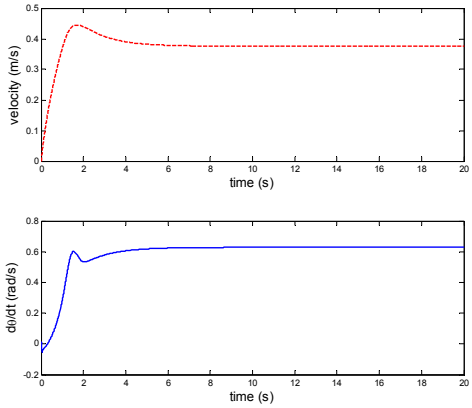

Fig. 4. USV absolute (top) and angular (bottom) velocities for reaching and tracking of the circular orbit

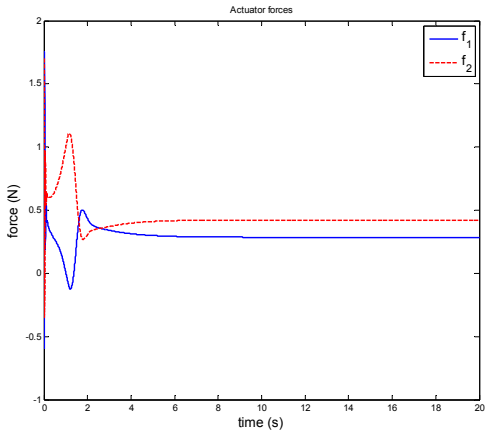

Fig. 5. Propeller control forces for reaching and tracking the circular orbit

$$m_{11} = 1.956 \pm .019 \quad m_{22} = 2.405 \pm .117 \quad m_{33} = .043 \pm .0068$$
$$d_1 = 2.436 \pm .023 \quad d_2 = 12.992 \pm .297 \quad d_3 = .0564 \pm .00085$$
$$\alpha_1 = 1.510 \pm .0075 \quad \alpha_2 = 1.747 \pm .013 \quad \alpha_3 = 1.592 \pm .0285$$

The trajectory parameters selected for the simulations are: x_o = .965 m, y_o = 1.27 m, r = .6 m, and $w(t)$ = .1 rev/s. Typical selected control parameters are η_1 = .1, η_2 = 10, and $\lambda_1 = \lambda_2$ = 2, though the effort parameters may need to be adjusted according to the actuator limits. The discontinuous "sign" functions were also replaced with continuous saturation functions of boundary layer thicknesses $\phi_1 = \phi_2$ = .1 (i.e., $\text{sgn}(S_i) \approx \text{sat}(\frac{S_i}{\phi_i})$, $i = 1,2$) to avoid chattering normally associated with sliding mode control [22-23].

Figure 2 presents the path of convergence of the transitional trajectories to the desired closed orbit from several different initial conditions. Figure 3 shows the convergence of position tracking of the controller to a target circular orbit for starting point 1. Figure 4 shows the smooth transition of the USV absolute and angular velocities to

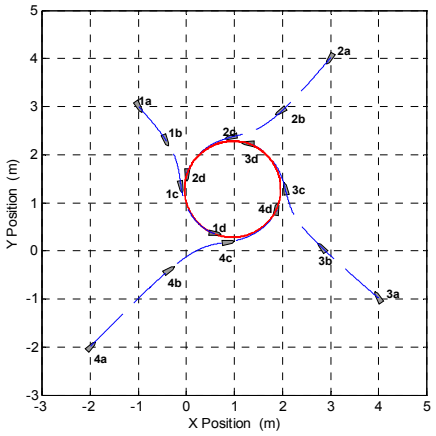

Fig. 6. Trajectory tracking and coordinated control of four USV's from the initial conditions: 1a, 2a, 3a, and 4a to the circular-orbit target. USV positions are shown at times: t_a=0s, t_b=2.5s, t_c=5s, and t_d=7.5s.

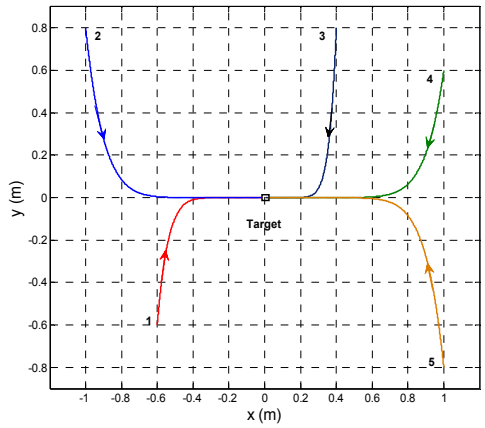

Fig. 7. Path tracking from five different starting points for a fixed point target

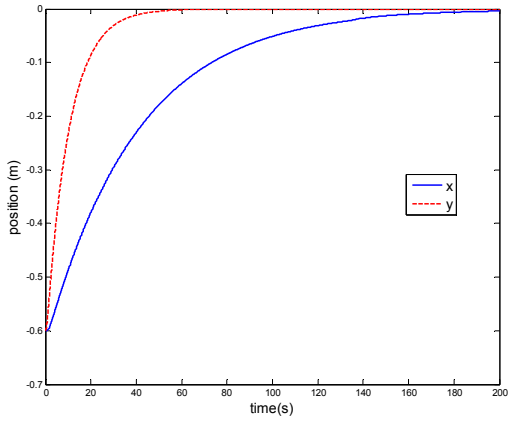

Fig. 8. USV position time history in inertial reference frame for a fixed point target

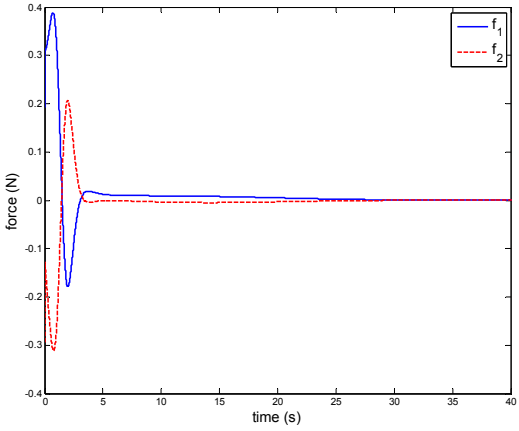

Fig. 9. Propeller control forces for reaching a fixed point target

constant values on the target circular trajectory. Figure 5 presents the two control (propeller) forces also smoothly converge to constant values at the target trajectory.

B. *Coordinated Control*

The second example demonstrates the coordinated control of four USV's, using the trajectories generated in section A. Figure 6 shows the coordinated control of four different USV's 1, 2, 3, and 4 starting from different initial positions at the same time t_a=0. The position of the USV's at times: t_b=2.5^s, t_c=5^s, and t_d=7.5^s are also shown and marked with the corresponding letters "b", "c", and "d". The ODE's in the Eq. (16), represent a Lipcshitz map, and satisfy the Existence and Uniqueness conditions of the solution. Hence, there is no possibility of collision among the USV's starting at different times or from different initial positions, by appropriately selecting the trajectory parameters and disregarding the size and the shape of the vessels. Note that according to section A, any isolated closed orbit could be used as a limit cycle for coordinated control.

C. *Fixed Set Point*

The third example demonstrates convergence of the same USV to the origin from an arbitrary initial condition. The desired state trajectory is a dynamic system with a stable node on the equilibrium point:

$$\begin{cases} \dot{x}_1(t) = -a_1 x_1(t) \\ \dot{x}_2(t) = -a_2 x_2(t) \end{cases}$$

where $x_1(t) = x(t) - x_\circ$ and $x_2(t) = y(t) - y_\circ$ are the state variables of the transitional trajectory and the constants a_1 and a_2 specify the speed of the exponential decay to the fixed point. The trajectory and control parameters are x_o = 0 m, y_o = 0 m, a_1 = .025 a_2 = .1, $\eta_1 = \eta_2$ = .1, $\lambda_1 = \lambda_2$ = .5, and $\phi_1 = \phi_2$ = .1 where again boundary layers are used to define a continuous approximation of the "sign" functions to avoid chattering.

Figure 7 presents the path of convergence of the transitional trajectories to the desired fixed point from five different initial conditions. Figure 8 shows the convergence

of position tracking of the controller to the origin for starting point 1. Figure 9 shows the smooth convergence of the two control forces to zero at the target fixed point where the plots are shown only the first 40 seconds for clarity.

VI. Conclusions

A method for combined smooth trajectory planning, tracking, and coordinated control is presented. The trajectory tracking control law is based on a sliding mode control approach where a transitional trajectory is defined by using ordinary differential equations in terms of the two position state feedbacks which smoothly converges to the desired target trajectory. A closed circular orbit, coordinated control of multiple vessels, and a fixed set point problem are used as examples to demonstrate the transitional trajectory planning and the effectiveness of the control law in tracking both the transitional and desired target trajectories.

Acknowledgements

This research was partially supported by the Office of Naval Research under the ONR Grant number N00014-04-1-0642. Support for this work from the Center for Nonlinear Dynamics and Control (CENDAC) at Villanova University is also acknowledged.

References

[1] Reyhanoglu, M., "Exponential stabilization of an underactuated autonomous surface vessel", *Automatica*, v 33, n 12, 1997, p 2249-2254.

[2] Kim, T.-H., Basar, T., and Ha, I.-J., "Asymptotic stabilization of an underactuated surface vessel via logic-based control" *American Control Conference*, 2002, p 4678 – 4683.

[3] Mazenc, F., Pettersen, K., and Nijmeijer, H., "Global uniform asymptotic stabilization of an underactuated surface vessel," *IEEE Transactions on Automatic Contro*l, v 47, n 10, 2002, p 1759-1762.

[4] Soro, D., and Lozano, R., "Semi-global practical stabilization of an underactuated surface vessel via nested saturation controller," *Proceedings of the American Control Conference*, Denver, CO, v 3, 2003, p 2006-2011.

[5] Dong, W., and Guo, Y, "Global time-varying stabilization of underactuated surface vessel," *IEEE Transactions on Automatic Control*, v 50, n 6, 2005, p 859-864.

[6] Peterson, K.Y., Mazenc, F., and Nijmeijer, H., "Global Uniform Asymptotic Stabilization of an Underactuated Surface Vessel: Experimental Results," *IEEE Transactions on Control Systems Technology*, v 12, n 6, 2004, p 891-903.

[7] Indiveri, G., Aicardi, M., and Casalino, G., "Nonlinear time-invariant feedback control of an underactuated marine vehicle along a straight course", *Proceedings of 5th Conference on Maneuvering and Control of Marine Craft (MCMC 2000)*, Aalborg, Denmark, 2000.

[8] Godhavn, J.-M., 1996, "Nonlinear Tracking of Underactuated Surface Vessels", *Proceedings of the IEEE Conference on Decision and Control*, Kobe, Japan, 2000.

[9] Pettersen, K.Y., and Nijmeijer, H., "Tracking control of an underactuated surface vessel" *Proceedings of the IEEE Conference on Decision and Control*, 1998, p 4561-4566.

[10] Encarnacao, P., and Pascoal, A., "Combined trajectory tracking and path following: An application to the coordinated control of autonomous marine craft," *40th IEEE Conference on Decision and Control* (*CDC*), Orlando, FL, v 1, 2001, p 964-969.

[11] Olfati-Saber, R., "Exponential epsilon -tracking and epsilon -stabilization of second-order nonholonomic SE (2) vehicles using dynamic state feedback," *Proceedings of the American Control Conference* (*IEEE Cat. No.CH37301*), v 5, 2002, p 3961-3967.

[12] Aguiar, A.P., and Hespanha, J.P., "Position tracking of underactuated vehicles," *Proceedings of the American Control Conference*, v 3, 2003, p 1988-1993.

[13] Behal, A., Dawson, D. M., Dixon, W.E., and Fang, Y., "Tracking and regulation control of an underactuated surface vessel with nonintegrable dynamics," *IEEE Transactions on Automatic Control*, v 47, n 3, 2002, p 495-500.

[14] Jiang, Z.-P., "Global tracking controller design for underactuated ships," *Proceedings of the IEEE Conference on Control Applications*, Mexico City, 2001, p 978-983.

[15] Toussaint, G. J., Basar, T., and Bullo, F., "Tracking for nonlinear underactuated surface vessels with generalized forces," *Proceedings of the IEEE International Conference on Control Applications*, Anchorage, AK, v 1, 2000, p 355-360.

[16] Lefeber, E., Pettersen, K. Y., and Nijmeijer, H., "Tracking control of an underactuated ship," *IEEE Transactions on Control Systems Technology*, v 11, n 1, 2003, p 52-61.

[17] Ashrafiuon, H., Muske, K. R., McNinch, L., and Soltan , R., "Sliding Model Tracking Control of Surface Vessels," *IEEE Transactions on Industrial Electronics SS on Sliding Mode Control in Industrial Applications* , to appear in Nov. 2008 issue.

[18] Ashrafiuon, H., and Muske, K., "Sliding Mode Tracking Control of Surface Vessels," *Proceedings of the American Control Conference*, Seattle, WA, 2008, p. 556-561.

[19] Muske, K., Ashrafiuon, H., Haas, G., McCloskey, R., and Flynn, T., "Identification of a Control Oriented Nonlinear Dynamic USV Model,"*Proceedings of the American Control Conference*, Seattle, WA, 2008, p. 562-567.

[20] Utkin, V. I., "Variable structure systems with sliding modes," *IEEE Transactions on Automatic Control*, v 22, 1977, p 212-222.

[21] Fossen, T. I., "Guidance and control of ocean vehicles," John Wiley & Sons, New York, NY, 1994.

[22] Slotine, J.-J. E., and Li, W., "Applied Nonlinear Control," Englewood Cliffs, NJ: Prentice Hall, 1991.

[23] H. K. Khalil. *Nonlinear Systems*. Prentice-Hall, Upper Saddle River, NJ, 1996, p 552-579.